JOURNAL OF CATALYSIS 19, 162–171 (1970)

Catalytic Decomposition of Sodium Chlorate

T. WYDEVEN

Ames Research Center, NASA, Moffett Field, California 94035

Received February 19, 1970

Thermogravimetry (TG) and differential scanning calorimetry (DSC) were used to study the catalytic decomposition kinetics of sodium chlorate. Cobalt oxide (Co_3O_4) preparations of known crystal structure, particle size, surface area, electrical conductivity, and chemical composition were used for catalysts. Co_3O_4 powder prepared from cobalt carbonate was found to be a sufficiently active catalyst to initiate decomposition of solid $NaClO_3$ as well as sodium perchlorate. As much as 60% of the total amount of $NaClO_3$ decomposed was found to occur in the solid state with 6.84% Co_3O_4 using TG at various heating rates. A change in phase from solid to liquid $NaClO_3$ was accompanied by an increase in the catalytic decomposition rate. The Freeman–Rudloff mechanism for the decomposition of chlorates is used to explain the high activity of the *p*-type semiconductor, Co_3O_4. The apparent activation energy for the catalytic decomposition of solid $NaClO_3$ increased from 28.5 to 47.6 kcal/mole in the range from 5 to 50% decomposition with 6.84% catalyst. Gamma preirradiation of the catalysts in air decreased their activity. There was no evidence of an induction period in the catalytic decomposition of solid $NaClO_3$ thus showing rapid nucleation of decomposition. The average measured heat of fusion of $NaClO_3$ using DSC was 5330 cal/mole with an average deviation of ±144 cal/mole.

Introduction

Sodium chlorate is a potentially useful chemical for storage and supply of oxygen in portable life support systems and therefore its decomposition kinetics is of interest.

Although intermediate reactions are reported to occur during the thermal decomposition of $NaClO_3$ (*1*, *2*) the overall reaction occurs as follows:

$$2NaClO_3(s) \rightarrow 2NaCl(s) + 3O_2(g) \qquad (1)$$

Markowitz *et al.* (*1*) reported that a slight trace of chlorine evolved during the decomposition of $NaClO_3$; however, Solymosi and Bansagi (*2*) found neither chlorine nor chlorine dioxide even in traces. Uncatalyzed $NaClO_3$ melts at 263°C and begins to decompose rapidly at about 465°C (*1*). Sodium chlorate, when mixed with 10 mole % manganese dioxide catalyst, decomposes at about 300°C, i.e., above the melting point, but at a much lower temperature than uncatalyzed $NaClO_3$ (*1*).

Freeman and Rudloff (*3*) studied the catalytic activity of several metal oxides for the thermal decomposition of potassium chlorate. They found that oxides of cobalt (CoO and Co_3O_4), which are generally *p*-type semiconductors, were effective catalysts for $KClO_3$ decomposition. Solymosi and Krix (*4*) found nickel oxide and lithium-doped nickel oxide, also *p*-type semiconductors to be good catalysts for $KClO_3$ decomposition.

This paper reports on the catalytic decomposition of $NaClO_3$ using Co_3O_4 catalysts which have been characterized in terms of their chemical compositions, crystal structure, surface area, particle size, and electrical conductivity. Some of the Co_3O_4 catalysts were sufficiently active to permit acquisition of kinetic data for the decomposition of solid $NaClO_3$. The influence of gamma preirradiation of the catalyst on its activity was also studied. Thermogravimetry (TG) and differential scanning calorimetry (DSC) were used to study the reaction kinetics.

Methods

Catalyst preparation. Cobalt oxide (Co_3O_4) catalysts were prepared by thermal decomposition of cobalt carbonate and of cobalt nitrate in air. Cobalt carbonate was prepared by precipitation of solutions of reagent grade cobalt nitrate hexahydrate with anhydrous sodium carbonate. The precipitated carbonate was decomposed to Co_3O_4 by heating in a muffle furnace for 24 hr at 338°C. The oxide was then ground lightly with an agate mortar and pestle and stored in a desiccator over anhydrous calcium sulfate.

Cobalt oxide catalysts were prepared from the nitrate by thermal decomposition of cobalt nitrate hexahydrate at 691°C for 20 hr. The sample was ground lightly midway in the heating cycle and finally stored in a desiccator over anhydrous calcium sulfate. Hereafter, the catalyst prepared from cobalt carbonate will be referred to as catalyst I and the catalyst prepared from cobalt nitrate as catalyst II. Preirradiation of the catalysts with gamma rays was done in air using ^{60}Co.

Equipment. TG and DSC data were gathered using a Perkin-Elmer thermal analysis system in conjunction with a strip-chart recorder. Samples were contained in quartz pans for both TG and DSC experiments and the reference used for the calorimetric measurements was an empty quartz pan. The average sample size used for TG was 3.94 mg. Prepurified nitrogen (stated purity 99.99%) was passed over the samples at about 30 ml/min during TG and 22 ml/min during DSC experiments.

BET surface area measurements were made at the temperature of liquid nitrogen using krypton as the adsorbate. It was assumed that the area occupied by a krypton molecule was 20.2 $Å^2$.

Debye-Scherrer X-ray powder photographs of the catalysts were taken using molybdenum $K\alpha$ radiation ($\lambda = 0.71069$ Å). Particle size measurements were taken from electron micrographs with the aid of a Carl Zeiss particle size analyzer.

Electrical conductivity measurements of the catalysts were made at 1 kHz using a General Radio Impedance Bridge (Model No. 1650A) and a conductivity cell fabricated from a glass syringe. The electrodes were platinum and were spring loaded. The syringe was placed in a larger Pyrex tube with electrical lead-throughs and stopcocks to allow for a continuous flow of gas through the outer tube. Small holes were bored through the syringe to allow entry of the surrounding gas atmosphere to the catalyst. All gases used during the conductivity measurements were predried with silica gel. The oxygen used was aviator's grade (stated purity 99.5%). The nitrogen was prepurified and helium was Liquid Carbonic Grade A. The electrical conductivity, σ, was computed using the following equation: $\sigma = 1/RA$ where R is the measured ac resistance (ohms); l, the distance between electrodes (cm); and A, the electrode area (cm^2).

Preparation of catalyst–reactant mixtures. Matheson, Coleman, and Bell Reagent Grade $NaClO_3$ was recrystallized once from distilled water before being dried at 110°C, ground with an agate mortar and pestle and then sieved. The sieve fraction less than 200 mesh was retained for kinetic experiments. G. Frederick Smith anhydrous sodium perchlorate was ground without recrystallization and sieved; the sieve fraction less than 200 mesh was retained and dried at 110°C before storage. After the appropriate amounts of $NaClO_3$ or $NaClO_4$ and catalyst were weighed, the two were mixed for 2 min in an agate vial with the aid of a Wig-L-Bug. The mixtures were stored in a desiccator over anhydrous calcium sulfate.

Results and Discussion

The crystallinity of catalysts I and II was revealed by sharply defined X-ray powder photographs. The d-spacings and relative intensities obtained from the powder photographs of both catalysts, despite differences in composition (see Table 1), agreed well with the data reported for Co_3O_4 (*5*). For example, the d-spacings for catalyst I deviated an average of ±0.016 Å from the recorded values.

Table 2 gives the BET surface area and

TABLE 1
CHEMICAL ANALYSIS OF CATALYSTS

Catalyst	Constituent	Wt (%)
Catalyst I	Co	69.12
	O	29.45
	NO_3^-	0.040
	CO_3^{2-}	0.89
	Na	0.069
	H_2O	1.45
Catalyst II	Co	75.71
	O	26.04
	NO_3^-	0.17
	H_2O	0

particle size of the $NaClO_3$, $NaClO_4$, and catalysts used in this study. Since the electron micrographs revealed that particles of catalysts I and II were irregularly shaped agglomerates or aggregates of nearly spherical crystallites, the particle sizes given in Column 4, Table 2, pertain to the mean agglomerate diameter. The crystallites of catalyst I, however, were more uniform in size than those of catalyst II as revealed by the micrographs. The mean diameter of the crystallites of catalyst I, also obtained from electron micrographs, was about 0.03 μ (i.e., the lower limit of the range of particle diameters, Column 5, Table 2), which agrees in magnitude with the particle size calculated from the BET surface area (see Table 2). An estimate of the crystallite size for catalyst II was not warranted because of the nonuniform crystallite size.

To determine the type of semiconductivity of catalysts I and II, ac conductivity measurements were made at 1 KHz as a function of temperature (from 135 to 255°C for catalyst I and from 135 to 315°C for catalyst II) in both nitrogen and oxygen atmospheres at about 760 Torr. On the assumption that adsorbed oxygen withdraws electrons from the catalyst, thus increasing the number of positive holes, it was expected that a *p*-type semiconductor would be more conductive in an oxygen than in a nitrogen atmosphere. Conductivity measurements revealed that catalysts I and II were significantly more conductive in oxygen compared to nitrogen which confirmed that both catalysts were *p*-type semiconductors. For example, at 198°C catalyst I had an ac electrical conductivity of 0.0141 mhos in oxygen and 0.00352 mhos in nitrogen while catalyst II had a conductivity of 0.00238 mhos in oxygen and 0.00113 mhos in nitrogen. The conductivity data also revealed that catalyst I was about three times more conductive in nitrogen and six times more conductive in oxygen than catalyst II. The higher conductivity of catalyst I in either a nitrogen or oxygen atmosphere may be attributed to its O/Co ratio (see Table 1) or to better intergranular contact in the packed powder.

The activity of catalysts I and II for $NaClO_3$ decomposition is shown by the TG curves presented in Fig. 1. Shown also in Fig. 1, for comparison, is a portion of a TG curve for the uncatalyzed decomposition of $NaClO_3$. It is evident from these curves that the onset decomposition temperature of $NaClO_3$, i.e., 391°C, has been depressed about 205°C by only 6.84 wt % of catalyst I and only 124°C by 18.44 wt % of catalyst II. The onset of decomposi-

TABLE 2
BET SURFACE AREA AND PARTICLE SIZE

Compound	BET surface area (m^2/g)	Mean particle diam (μ)		Particle diam range obtained from electron micrographs (μ)
		Calc from surface area[a]	From electron micrographs	
Catalyst I	67	0.015	0.52	0.029–2.5
Catalyst II	0.75	1.3	1.8	0.18–3.6
$NaClO_3$	0.16	16	—	—
$NaClO_4$	0.25	9.7	—	—

[a] Assuming spherical particles.

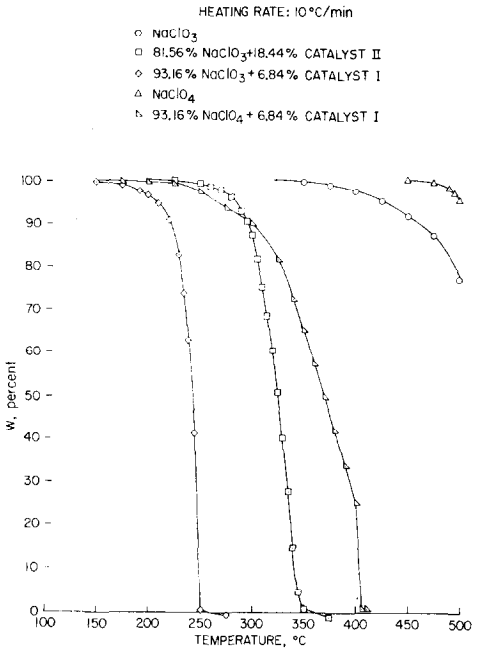

FIG. 1. TG curves of catalyzed and uncatalyzed sodium chlorate and sodium perchlorate.

tion was taken as the temperature at which 2% (or $W = 98\%$, where W is the percentage of unreacted $NaClO_3$) of the sample had decomposed (*1*) at the experimental heating rate. It was first assumed that $NaClO_3$ decomposed according to Eq. (1) in order to calculate the extent of decomposition from the TG data. The total sample weight loss upon completion of several TG experiments, some with and some without catalysts, agreed within $\pm 0.75\%$ with the expected weight loss based on Eq. (1).

Although minor changes in catalyst composition, such as a change in stoichiometry, may have occurred within the uncertainty of the weight loss measurements, the word catalyst will still be used to describe the cobalt oxides. The word catalyst will be used because a catalytic effect on the rate of $NaClO_3$ decomposition was obvious, Fig. 1, when the chlorate was mixed with the cobalt oxides.

Although the overall decomposition of $NaClO_3$ is described by Eq. (1), it has been reported (*1*, *2*, *6*) that $NaClO_3$ decomposes in more than one step with one of the intermediate steps being the disproportionation reaction:

$$4NaClO_3(s) \rightarrow 3NaClO_4(s) + NaCl(s), \quad (2)$$

followed by $NaClO_4$ decomposition. Therefore, it was also of interest to investigate the effect of catalyst I on $NaClO_4$ decomposition (see Fig. 1). For comparison with catalyzed $NaClO_4$ decomposition, a partial decomposition curve of uncatalyzed $NaClO_4$ is also shown in Fig. 1. The onset decomposition temperature of uncatalyzed $NaClO_4$ (i.e., 489°C) has been depressed 246°C by 6.84% of catalyst I. In addition, Fig. 1 reveals that $NaClO_4$ is more stable than $NaClO_3$.

The high reactivity of catalyst I versus catalyst II, for $NaClO_3$ decomposition (see Fig. 1), might be attributed to the greater surface area and/or electrical conductivity (assuming electron transfer is involved in the rate limiting step) of catalyst I. It is difficult to distinguish the relative importance of surface area and electrical conductivity because the specific surface conductivity of powdered catalysts is also a function of structural factors (e.g., surface area and particle size). Therefore, a comparison of the measured conductivity of catalysts I and II has little significance since the surface area and particle size are greatly different (*7*).

Solymosi and Krix (*4*), working with powdered NiO catalysts sintered at different temperatures and used for catalyzing the decomposition of $KClO_3$, suggested that surface area played a minor role in NiO activity and the electrical properties were more important. NiO sintered at 500°C was reported to be three times more conductive, and was also found to be a better catalyst than NiO sintered at 1000°C. However, no surface area measurements were reported.

The high activity of *p*-type semiconductors, such as catalyst I, versus *n*-type for example, MnO_2 and Fe_2O_3 for chlorate decomposition [with 8.3 wt % MnO_2 catalyst, the onset decomposition temperature of $NaClO_3$ was 300°C (*1*) compared to 186°C with 6.84% catalyst I, the "initial" decomposition temperature of $KClO_3$ was 400°C with 12 wt % Fe_2O_3 compared to 335°C with 5.8% of the *p*-type semicon-

ductor CoO (*3*).], may be explained on the basis of the reaction scheme and mechanisms proposed by Freeman and Rudloff (*3*) for the catalytic decomposition of $KClO_3$. These authors suggest the following reaction steps:

1. $ClO_3^- + e(\text{solid catalyst}) \rightarrow ClO_2^- + O^-(\text{ads})$,
2. $O^-(\text{ads}) \rightarrow O(\text{ads}) + e(\text{solid catalyst})$,
3. $2O(\text{ads}) \rightarrow O_2(\text{gas})$,
4. $O(\text{ads}) + O^-(\text{ads}) \rightarrow O_2(\text{gas}) + e(\text{solid catalyst})$,

where step 2 is rate limiting. [The chlorite formed in step 1 may then either rapidly decompose or disproportionate at the temperatures of $NaClO_3$ decomposition as suggested by Solymosi (*8*).] Step 2 was taken as the rate-limiting step because the activity of several metal oxide catalysts for $KClO_3$ decomposition was found to increase in the same order as the ability of the higher valent catalyst cations to accept electrons and thus be reduced to a lower valence, e.g., $Mn^{4+} + 2e \rightarrow Mn^{2+}$. A *p*-type semiconductor would favor step 2 because of the presence of positive holes in *d*-orbitals which would be available to accept an electron from an adsorbed oxide ion. Dowden (*9*) also stated that for oxygen reactions the most active oxides are the p_d-type, i.e., where vacancies occur in *d*-orbitals.

Although a change in cobalt oxide stoichiometry during catalytic decomposition cannot be ruled out, it is doubtful, based on the electrical conductivity data of Duquesnoy (*10*) that this change would convert the catalyst from a *p*- to *n*-type semiconductor. Duquesnoy has shown that the electrical conductivity of Co_3O_4 continuously decreases at 1000°C (without an apparent inflection point) with a decrease in oxygen pressure from 1 to 10^{-12} atm. At 10^{-12} atm, the conductivity suddenly increases due to cobalt metal formation.

Figure 2 shows the influence of catalyst I concentration on the decomposition of $NaClO_3$. From the data in both Figs. 1 and 2 it is evident that adding 6.84% of catalyst I (see Fig. 1) lowered the onset

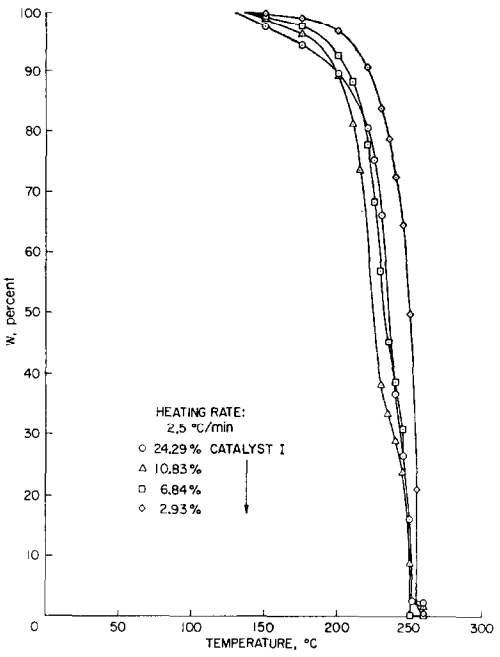

FIG. 2. TG curves showing the influence of catalyst concentration on the decomposition rate of sodium chlorate.

decomposition temperature of $NaClO_3$ 205°C; but a much larger amount of catalyst I, i.e., 24.29%, lowered the onset decomposition temperature only 26°C more (see Fig. 2). The onset decomposition temperature was only 19°C higher with 2.93% than with 6.84% of catalyst I (see Fig. 2).

Figure 2 also shows that the rate of decomposition is slower, beginning at about $W = 96\%$, for the sample containing 24.29% catalyst than for samples containing either 6.84 or 10.83%. To explain this unexpected behavior the following experiment was performed. Separate samples containing 6.84 and 24.29% catalyst were heated at 2.5°C/min to 236°C and maintained at this temperature for the remainder of the experiment (see Fig. 3). The data in Fig. 3 confirm the greater rate of decomposition during the initial heating period for the sample with 24.29% catalyst. The rate of decomposition of the 6.84% catalyst sample increases until it is greater than the 24.29% catalyst sample above 210°C. The new information revealed in

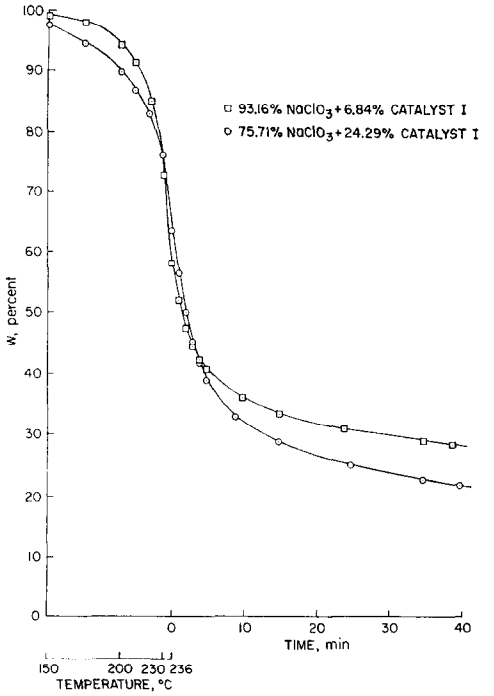

FIG. 3. TG (2.5°C/min heating rate) followed by isothermal weight-change (236°C) curves for high and low catalyst loadings. Note the fall-off in rate at 236°C for low catalyst loading and higher rate at high catalyst loading.

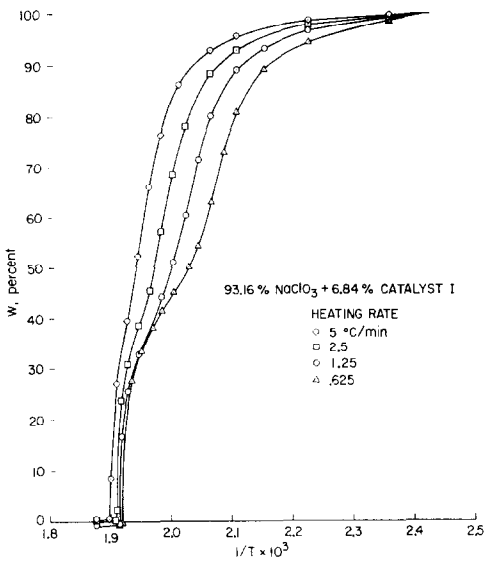

FIG. 4. TG curves showing the effect of heating on the catalytic decomposition of sodium chlorate. Note deceleration in rate near $W = 40\%$.

Fig. 3 is that a higher decomposition rate is maintained by the higher percentage of catalyst sample at 236°C, resulting in more extensive decomposition at the steady temperature condition. Thus, the crossing over by the high percentage catalyst curve in Fig. 2 may indicate a thermal lag caused by filling the void volume with catalyst and reducing interparticle contacts between the relatively large chlorate particles. The significant difference in particle size between the $NaClO_3$ and catalyst I (see Table 2) allows voids in the chlorate to be filled by the smaller catalyst particles.

A characteristic feature of the decomposition rates of catalyst I–$NaClO_3$ mixtures, when heated at 5°C/min or less, was a transient deceleration in rate around $W = 40\%$ (e.g., see Fig. 4). Both TG and DSC curves (see Fig. 5) revealed this effect. (Since reactions 1 and 2 are exothermic by —12.5 and —7.96 kcal/mole (*2*), respectively, deceleration in the rate of $NaClO_3$ decomposition is evidenced by a decrease in rate of heat evolution when DSC is used.) It can be deduced from the DSC curve for a 6.84% catalyst I–$NaClO_3$ mixture that deceleration begins at about 240°C followed by rapid acceleration start-

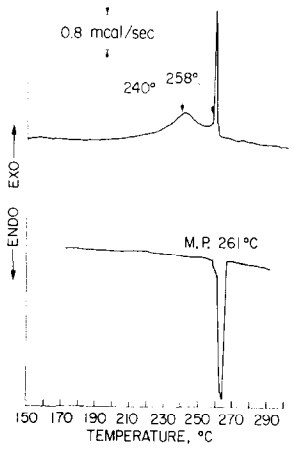

FIG. 5. DSC curves of catalyzed and uncatalyzed sodium chlorate: (upper) 93.16% $NaClO_3$ + 6.84% catalyst I; sample size, 2.257 mg; heating rate, 5°C/min (lower) $NaClO_3$; sample size, 2.194 mg; heating rate, 5°C/min.

ing at 258°C at a heating rate of 5°C/min. Using TG and a heating rate of 5°C/min, deceleration started at about 248°C and acceleration started at 254°C with a 6.84% catalyst I–$NaClO_3$ mixture.

Deceleration in the decomposition rate of solid $NaClO_3$ which is apparent from the TG and DSC data may be due to several factors. Deceleration may result from the partial conversion of $NaClO_3$ to the more stable $NaClO_4$ in the solid phase by reaction 2. The greater stability of $NaClO_4$ is evidenced by data in Fig. 1. Other factors that could account for the observed deceleration in rate of decomposition are: (a) a decrease in catalyst activity as decomposition progresses; (b) a decrease in the flux of chlorate ions to the catalyst surface; and (c) a change in reaction mechanism. A decrease in chlorate ion flux could be due to the accumulation of $NaClO_4$ and a continuous increase in the thickness of the product layer surrounding unreacted $NaClO_3$.

The acceleration in rate which follows deceleration may result from melting of unreacted $NaClO_3$. DSC curves for catalyzed and uncatalyzed $NaClO_3$ (see Fig. 5) also provide evidence that acceleration occurs in the region of melting. Melting of uncatalyzed $NaClO_3$ occurs at 261°C (lower curve Fig. 5), whereas acceleration in the catalyzed decomposition of $NaClO_3$ begins at 258°C (upper curve Fig. 5). The melting point of $NaClO_3$ found by DSC agrees within experimental error (±2°C) with the reported melting point of 263°C (*1*).

Markowitz *et al.* (*1*) also found that alkali chlorate–MnO_2 mixtures decomposed rapidly following liquefaction. They ascribed this rapid decomposition to increased anion mobility (i.e., the Hedvall Effect). It was further reported that the liquid phase decomposition of $KClO_4$ was about 50 times faster than the corresponding solid phase rate (*1*). Since $NaClO_4$ is a product of $NaClO_3$ decomposition via reaction 2, it is expected, by analogy to $KClO_4$, that $NaClO_4$ would also decompose more rapidly in the liquid phase or in molten $NaClO_3$.

It should also be noted in Fig. 4 that acceleration begins near 254°C, i.e., about 7°C lower than the melting point of pure $NaClO_3$, which is a reasonable melting point for a mixture of NaCl, $NaClO_4$, and unreacted $NaClO_3$.

The explanation offered for the acceleration in rate would also explain why the TG curves at various heating rates converge around 250°C (see Fig. 4), i.e., the catalytic decomposition rate in the liquid phase is very fast and almost independent of the heating rate.

In comparing the two DSC curves of catalyzed and uncatalyzed $NaClO_3$ (see Fig. 5), it is apparent from the heat evolved prior to melting (see upper curve, Fig. 5) that catalyst I is sufficiently active to initiate decomposition of solid $NaClO_3$.

Since uncatalyzed $NaClO_3$ melts without decomposition, it was possible to obtain the heat of fusion by DSC. The average measured heat of fusion was 5330 ± 144 cal/mole. This is apparently the first reported value for the heat of fusion of $NaClO_3$.

Melting may also explain the acceleration in rate near 400°C ($W = 25\%$) of $NaClO_4$ (see Fig. *1*). The melting point reported for $NaClO_4$ is 471°C (*8*). The low temperature at which acceleration occurs relative to the melting point of $NaClO_4$ may be due to the formation of a low melting mixture of the products of $NaClO_4$ decomposition. Some support for this argument is obtained from the data of Solymosi (*8*). He found that a mixture of 70 mole % $NaClO_4$ and 30 mole % NaCl melted at 415°C, which is 56°C below the melting point of pure $NaClO_4$.

It also appears that the primary action of Co_3O_4 is to catalyze reaction (1) and not (2). If reaction (2) were catalyzed, a large extent of decomposition below about 250°C would not be expected because of the formation of the more stable $NaClO_4$. Figure 1 shows that decomposition of $NaClO_4$ with 6.84% Co_3O_4 catalyst begins slowly at about 243°C and does not accelerate until above 300°C; whereas the catalytic decomposition of $NaClO_3$ is already complete at about 250°C, when both

are compared at the same heating rate (10°C/min).

The activity of catalyst I for decomposing solid $NaClO_3$, after a layer of product has accumulated between unreacted $NaClO_3$ and the catalyst, can be accounted for by diffusion of chlorate ions to the catalyst surface. If one assumes that the catalytic decomposition of $NaClO_3$ is analogous to a solid–solid reaction, then the criterion stated by Rees (*11*) for bulk diffusion in solid–solid reactions can be applied to the solid–catalyst reaction. He stated that solid–solid reactions involving bulk phase diffusion take place at temperatures $> 0.52\ T_m$, where T_m is the melting point (°K). If 261°C is taken as the melting point for $NaClO_3$ (see Fig. 5), then $0.52\ T_m$ equals 278°K (5°C) which is far below the onset decomposition temperature, i.e., 186°C of catalyst I–$NaClO_3$ mixtures (see Fig. 1). Therefore, chlorate ions should be sufficiently mobile to diffuse through the product layer to the catalyst surface and subsequently decompose, possibly via the Freeman–Rudloff mechanism.

Ozawa (*12*) has described a method which was used previously by the author (*13*) for deriving kinetic parameters from TG data. A plot of W versus $1/T$ for different heating rates is convenient for deriving the activation energy at different extents of reaction from TG data by the Ozawa method (see Fig. 4). The apparent activation energy derived from the data in Fig. 4, at different extents of decomposition of solid $NaClO_3$, is shown in Table 3. The continuous increase in apparent activation as decomposition proceeds, Table 3, did not permit a determination of the reaction order or preexponential factor by the Ozawa method.

TABLE 3
APPARENT ACTIVATION ENERGY FOR THE CATALYTIC DECOMPOSITION OF SOLID $NaClO_3$

W (%)	E(kcal/mole)[a]
95	28.5 ± 5.4
90	33.7 ± 2.0
80	36.1 ± 2.1
70	37.5 ± 3.5
60	39.7 ± 2.5
50	47.6 ± 3.6

[a] Uncertainties are for a 95% confidence interval.

There was no apparent correlation between the activation energy for conduction and the apparent activation energy for decomposition. The activation energies for conduction in both nitrogen and oxygen were consistently lower than the lowest apparent activation energy for decomposition. For example, for catalyst I the activation energy for conduction in a nitrogen atmosphere was 11.0 ± 1.4 kcal/mole, which is significantly lower than the apparent activation energy for decomposition in the same atmosphere (see Table 3). The lack of correlation between the activation energies may be due to a decrease in catalyst activity as reaction progresses. A decrease in catalyst activity may then cause the apparent activation energy for decomposition to be higher than the activation energy for conduction. A decrease in catalyst activity as reaction progresses may also account for the continuous increase in apparent activation energy, Table 3. In addition to electron transfer, diffusion of chlorate ions to the catalyst surface may also be a factor influencing the reaction rate and giving rise to a higher apparent activation energy for decomposition than for conduction.

A change in reaction mechanism from, for example, the Freeman–Rudloff mechanism to one in which the rate-controlling step does not include the oxide catalyst may also account for the continuous increase in the apparent activation energy. The following evidence supports a change in reaction mechanism from a catalytic reaction to a mechanism not involving the Co_3O_4 catalyst. Osada *et al.* (*6*), from their study of the uncatalyzed decomposition of liquid $NaClO_3$, reported an activation energy of 48.9 kcal/mole. The value reported by Osada *et al.* compares favorably with the apparent activation energy of 47.6 kcal/mole at 50% decomposition with catalyst I (see Table 3).

Gamma preirradiation in air of catalysts I and II (dose 5.0×10^6 R) was carried out and the activity of preirradiated and unir-

radiated catalysts was compared (see Fig. 6). The lower activity of preirradiated catalysts (shown only for samples containing 6.84% of catalyst I, Fig. 6) was characteristic of both catalysts I and II. Furthermore, it is apparent from Fig. 6 that the initial decomposition rate is the maximum rate for both irradiated and unirradiated catalysts.

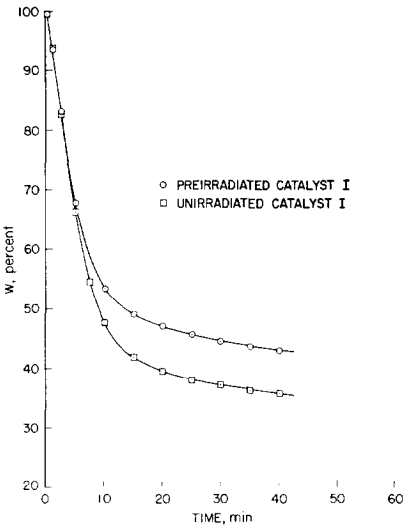

FIG. 6. Isothermal weight-change curves (220°C) showing influence of gamma preirradiation on catalyst activity. Unirradiated and irradiated sample composition: 93.16% $NaClO_3$ + 6.84% catalyst I.

[Weight loss determined by TG for preirradiated catalyst–$NaClO_3$ mixtures agreed, within experimental error, with the expected weight loss based on equation (*1*). Therefore, $NaClO_3$–preirradiated catalyst mixtures did not decompose at room temperature or prior to the start of a decomposition experiment.]

The behavior exhibited by preirradiated Co_3O_4 (Fig. 6) versus the unirradiated catalyst would be expected for a *p*-type oxide semiconductor if irradiation resulted in some surface decomposition with loss of oxygen. A more stoichiometric compound having fewer positive holes in *d*-orbitals would result from loss of oxygen, thus creating a catalyst of lower activity.

There was no evidence of an induction period in the decomposition of solid $NaClO_3$ in the presence of either preirradiated or unirradiated catalyst I at 220°C (see Fig. 6). The absence of an induction period indicates that nucleation of decomposition is rapid. The isothermal decomposition curves of $NaClO_3$ given by Solymosi and Bansagi (*2*) show induction periods of about 6 min at 466°C and 19 min at 457°C.

In summary, crystalline Co_3O_4 powder prepared by thermal decomposition of cobalt carbonate has been found to be an effective catalyst for the thermal decomposition of $NaClO_3$. The catalyst was sufficiently active at low concentrations to initiate decomposition of solid $NaClO_3$. A change in phase from solid to liquid $NaClO_3$ was accompanied by an increase in the catalytic decomposition rate. A reaction scheme has been cited which may explain the high activity of Co_3O_4, a *p*-type semiconductor. The *p*-type semiconductivity of the cobalt oxide was confirmed by ac conductivity measurements in different gas atmospheres. The Co_3O_4 catalysts prepared from cobalt carbonate also initiated decomposition of solid $NaClO_4$. The apparent activation energy for the catalytic decomposition of solid $NaClO_3$ increased from 28.5 to 47.6 kcal/mole as decomposition progressed. Reasons have been given that may explain the continuous increase in apparent activation energy. The higher value for the apparent activation energy obtained after 50% decomposition agrees with the value reported by others for uncatalyzed $NaClO_3$. There was no correlation between the apparent activation energy for decomposition and the activation energy for conduction. Several reasons have been given to explain the lack of correlation. Gamma preirradiation of Co_3O_4 lowered its activity for decomposing $NaClO_3$ and an explanation has been given for the observed behavior. No induction period was evident in the catalytic decomposition of $NaClO_3$.

ACKNOWLEDGMENT

The author is grateful for the suggestions of Dr. E. V. Ballou.

REFERENCES

1. MARKOWITZ, M. W., BORYTA, D. A., AND STEWART, H., JR., *J. Phys. Chem.* **68**, 2282 (1964).

2. SOLYMOSI, F., AND BANSAGI, T., *Acta Chim. Acad. Sci. Hung.* **56,** 337 (1968).
3. FREEMAN, E. S., AND RUDLOFF, W., Final Technical Report, U. S. Army Project IC 522301A060, Contract No. DA-18-035-AMC-341(A) (1967).
4. SOLYMOSI, F., AND KRIX, N., *Acta Chim. Hung. Tomus* **34,** 241 (1962).
5. *ASTM* X-Ray Powder Data File, Card No. 9-418.
6. OSADA, E., KUSAMOTO, K., AND MUKAI, K., *Kogyo Kayaku Kyokai-shi* **27,** 91 (1966).
7. BEVAN, D. J. M., SHELTON, J. P., AND ANDERSON, J. S., *J. Chem. Soc., London* **1948,** 1729.
8. SOLYMOSI, F., *Acta Chim. Hung. Tomus* **57,** 11 (1968).
9. DOWDEN, D. A., *in* "Chemisorption" (W. E. Garner, ed.), p. 5. Academic Press, New York, 1957. (Proceedings of a Symposium).
10. DUQUESNOY, A., *Rev. Hautes Temp. Refract.* **3,** 201 (1965).
11. REES, A. L. G., *in* "Chemistry of the Defect Solid State," p. 91. Wiley, New York, 1954.
12. OZAWA, T., *Bull. Chem. Soc. Jap.* **38,** 1881 (1965).
13. WYDEVEN, T., *J. Catal.* **16,** 82 (1970).